

**ANALYSIS OF CONTACT OF A RIGID SPHERE AGAINST A DEFORMABLE FLAT**

*Tomasz Trzepieciński<sup>1)\*</sup>, Łukasz Bąk<sup>1)</sup>, Feliks Stachowicz<sup>1)</sup>, Sergei Bosiakov<sup>2)</sup>, Sergei Rogosin<sup>3)</sup>*

*<sup>1)</sup>Rzeszow University of Technology, Faculty of Mechanical Engineering and Aeronautics, Rzeszów, Poland*

*<sup>2)</sup>Belarusian State University, Faculty of Mechanics and Mathematics, Minsk, Belarus*

*<sup>3)</sup>Belarusian State University, Department of Economics, Minsk, Belarus*

Received: 26.10.2015

Accepted: 11.11.2015

\* Corresponding author: *e-mail: tomtrz@prz.edu.pl, Tel.: +48 608 091 989, Department of Materials Forming and Processing, Faculty of Mechanical Engineering and Aeronautics, Rzeszow University of Technology, 8 Powstańców Warszawy Ave., 35-959 Rzeszów, Poland*

**Abstract**

In the paper the strain hardening effect on the contact of a rigid ball and elastic-plastic flat is considered using experiments and finite element method. The experiments were carried out for DC04 steel sheet metal. The flat samples of 20 mm width and 200 mm length were straightened using uniaxial tensile test to receive different strain values: 5, 10, 15, 20, 25 and 30%. The indentation tests were performed using a modified Zwick Roell Z030 operated in the compression mode. The diameter of bearing steel indenter was 6 mm. It was found that the strain hardening phenomenon and anisotropy of material have a great influence on the ball indentation value and the maximal indentation force. The linear dependence between the normal load and penetration depth was observed. Furthermore, it was found that the value of penetration depth for specific force value decreases non-linearly with the increase of sample strain. Pre-strained samples cut transverse to the rolling direction exhibit higher deformation resistance than samples cut along the rolling direction. The springback analysis in ABAQUS was executed for studying the actual indentation depth after the indenter is unloaded.

**Keywords:** elastic-plastic contact, finite element method, plastic deformation, strain hardening, surface roughness

**1 Introduction**

The elastic-plastic contact of two non-conforming bodies is a fundamental problem in the mechanics of materials [1]. When two rough solids are brought to contact under a normal preload, contact junctions are formed at their contacting asperity tips, which may deform elastically, elastic-plastic or plastic [2]. In metal forming operations, rough surfaces consist of asperities having different radii and height, so it is a difficult task to evaluate the contact area and contact load [3]. The modeling of elasto-plastic hemispheres in contact with a rigid surface is important in contact mechanics on both the macro and micro scales [4]. The case of a rigid spherical indentation of a deformable half-space has been thoroughly investigated experimentally [5] and numerically [1, 6, 7].

The contact mechanics study of rough surfaces is mostly based on the method of calculation of contact characteristics developed by the Greenwood and Williamson model [8]. Due to the mathematical complexity, most problems of contact mechanics are restricted to linear elastic or perfectly plastic cases [9]. Brizmer et al. [10] analysed the behaviour of an elastic-plastic contact

between a deformable sphere and a rigid flat under combined normal and tangential loading with full stick contact condition. Ovcharenko et al. [11] performed experimental investigation to calculate the real contact area between a sphere and a flat during loading–unloading, and cyclic loading–unloading in the elastic–plastic regime. Shankar and Mayuram [12] proposed a new empirical relations to determine the contact load and the contact area based on the results of the numerical analyses. Jackson and Green [13] studied statistically elasto-plastic contact between two rough surfaces using the results of own finite element analysis of an elasto-plastic sphere in contact with a rigid flat.

The effect of strain hardening on the elastic-plastic contact of a deformable sphere against a rigid flat under full-stick contact conditions was studied by Chatterje and Saho [14]. Chang et al. [15] proposed an elastic-plastic contact where the sphere remains in elastic contact until a critical interference is reached, above which the volume conservation of the sphere tip is imposed. In the microcontact model for the contact between two nominally flat surfaces analysed by Zhao et al. [16] the transition from elastic deformation to fully plastic flow of the contacting asperity is modelled, based on contact-mechanics theories. The effect of anisotropy on the pressure distribution and contact area, when an anisotropic half space is in contact with a rigid sphere is studied by Bagault et al. [17]. The study showed that the change of the Young's modulus along a direction parallel to the surface does not significantly affect the contact pressure distribution but the contact area is no more circular.

The finite element (FE) method can be used to calculate accurately the contact parameters like contact load, contact area, and pressure, and so forth, removing some of the assumptions made in the earlier analytical theories regarding asperity interaction [18]. One of the first works that provided an accurate result of elastic-plastic contact of a hemisphere and a rigid flat using FE was the study of Kogut and Etsion [19]. They concluded a negligible effect of strain hardening for the friction-less and the nonadhesive contact. Jackson and Green [20] observed the effect of the deformed geometry on the effective hardness and presented some empirical relations of contact area and contact load. Sathish Gandhi et al. [2] presented the effect of tangent modulus in a contact parameters of a spherical ball contact with a flat plate.

Leu [21] proposed an indentation model of the Brinell hardness test, which is a rigid ball-deformable plane contact model, to elucidate the sliding friction mechanism of sheet metal forming. In a proposed model, the friction force can be defined as a combination of shear and plough forces. In many industrial applications it assumed that the frictional behaviour is independent of the sliding direction. This assumption seems to be unrealistic and many experimental studies show that the frictional behaviour can change drastically with the sliding direction, requiring an anisotropic model [22].

In the paper the strain hardening effect on the contact of a rigid ball and elastic-plastic flat is considered using experiments and finite element method. We analysed the change in the surface topography of pre-strained sheet specimens cut along three directions with respect to the rolling direction. Furthermore, we studied the effect of strain hardening phenomenon and sample orientation on the value of indentation depth.

## 2 Experimental investigations

### 2.1 Material

Experiments were carried out for DC04 steel sheet metal. The mechanical properties of the sheet metal listed in Table 1 have been determined through uniaxial tensile tests along three directions with respect to the rolling direction. The strain hardening behaviour uses the Hollomon power-

type law expressed as  $\sigma = C \cdot \varepsilon^n$ , where parameters  $C$  and  $n$  (**Table 1**) in this Hollomon equation have been fitted on stress-strain curve of tensile test.

**Table 1** Mechanical properties of DC04 steel sheet

Orientation	Yield stress $R_{p0.2}$ MPa	Ultimate strength $R_m$ , MPa	Elongation $A_{50}$ , %	Hardening coefficient $C$ , MPa	Strain hardening exponent $n$	Lankford's coefficient $r$
0°	182.1	322.5	45.8	549.3	0.214	1.751
45°	196	336.2	41.6	564.9	0.205	1.124
90°	190	320.9	45.6	541.6	0.209	1.846
mean value	189.37	326.53	44.3	551.93	0.2093	1.5736

## 2.2 Methods

The friction properties of the deep drawing quality steel sheets used in the experiments were determined by using the pin-on-disc tribometer T01-M. In this method, the friction coefficient as a function of angular position with respect to the rolling direction of the sheet metal was measured. The method of friction determination is explained in recent papers of the authors [22, 23].

Continuous indentation tests were performed on DC04 steel sheets with a thickness of 2 mm. The samples for indentation tests were cut into three directions: along the rolling direction, at 45° to the rolling direction and transverse to the rolling direction. The flat samples of 20 mm width and 200 mm length were straightened using uniaxial tensile test to receive different strain values  $\varepsilon_i$ : 5, 10, 15, 20, 25 and 30%. Then the surface of pre-strained samples was grinded.

The indentation tests were performed using a modified Zwick Roell Z030 operated in the compression mode. The applied load versus the crosshead displacement or depth of the indentation were continuously recorded throughout the tests. A maximum load of 60, 80, 100, 125, 150, 200, 250, 300 N was applied for each sample. In our analyses, the indenter made of bearing steel has 6 mm diameter.

## 3 Numerical modeling

The symmetry of the process was exploited, in order to reduce computational time. Only one quarter of blank and the ball with symmetry boundary conditions were modelled. The geometry of the ball was assumed as discrete rigid. An elastic-plastic material model of sheet was implemented. The elastic behaviour is specified in numerical simulations by the value of Young's modulus,  $E = 210$  GPa and Poisson's ratio  $\nu = 0.3$ . In the numerical model, the anisotropy of the material has been established using the Hill yield criterion [24] which is the most frequently used yield function for steel sheet metals [25]. For the blank meshing the 3-dimensional 8-node brick elements were used.

The experimental results of friction tests show that the friction coefficient depends on the measured angle from the rolling direction, and corresponds to the surface topography. It was found that the plot of the friction coefficient as a function of angular position with respect to the rolling exhibits two maxima within a 360° rotation:  $\mu_1 = 0.142$  and  $\mu_2 = 0.157$ . In the numerical analysis of the contact of the rigid sphere against a deformable flat there are a small relate displacements of parts in contact. So, we assumed the isotropic value of the friction coefficient of 0.1495.

## 4 Results and discussion

### 4.1 Surface roughness

The values of the Ra and Rz parameters measured along the rolling direction ( $\parallel$ ) and transverse to the rolling direction ( $\perp$ ) of the sheet metal increased with the tensile strain level (**Fig. 1**). This dependence is nearly linear. As we found, the determination coefficient  $R^2$  between roughness parameters values and the strain value is higher than 0.9104. The linear character of this relation is confirmed by Stachowicz [26]. The increase in surface roughness of the sheet is the result of reorientation and fragmentation of the individual grains, mainly in the subsurface. Grain orientation fragmentation refers to the tendency for the lattice of different regions of a grain to rotate under the deformation toward a small number of distinctly different orientations [27]. The ball indentation with load up to 60 N caused a visible effect on the surface profile (**Fig. 2**).

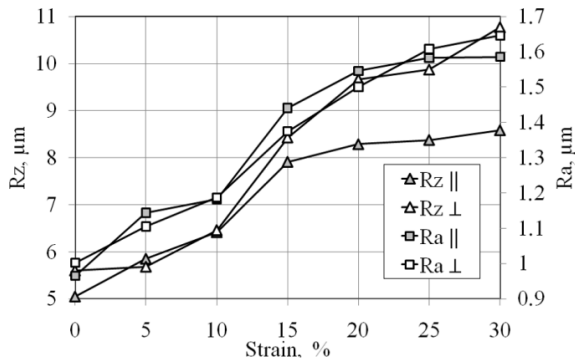


**Fig. 1** Effect of tensile strain on the change of the Ra and Rz parameters values of sheet surface

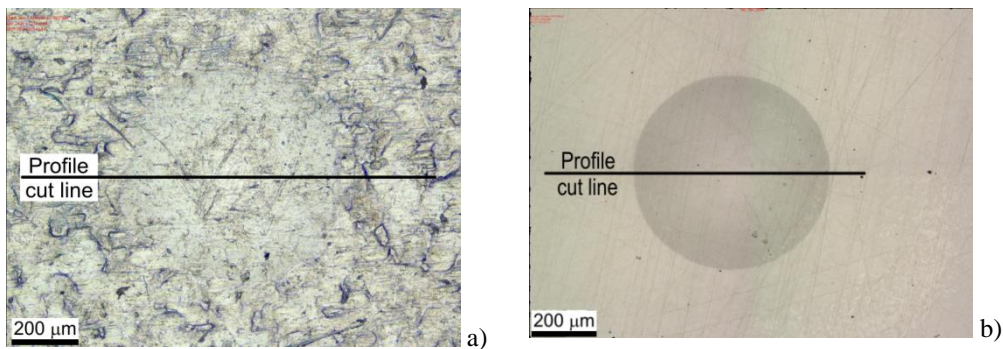


**Fig. 2** Optical micrograph of indentation for normal load 300 N: a) original surface, b) grinded surface

The values of indentation depth during testing non-prestrained sheets for normal loads 100 N and 200 N (**Fig. 3**) were smaller than the value of Rz parameter. This fact leads to the conclusion that only the asperities of the surface were deformed. Increasing the normal load to 300 N causes the plastic deformation occurring in the subsurface, some distance below the roughness profile. Evidently, the observed relationship between impression depth and the Rz parameter is different to pre-strained sheets due to the strain hardening effect. In the case of Ra parameter in the range of strain between 0 and 20% is observed a fast increasing of its value. After exceeding the value

of strain of 20% the value of Ra parameter measured at 0° and 90° according to the rolling direction increased a little (**Fig. 1**). Simultaneously, the value of Rz parameter constantly increases at the whole range of sample pre-strain. Strain hardening of surface roughness limits the change of roughness average Ra of the sheet as a result of uniaxial strain of the sample.

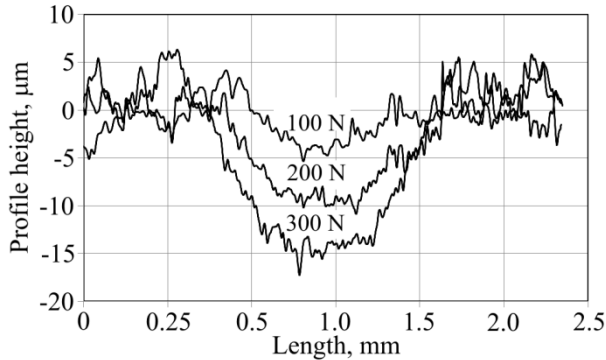


**Fig. 3** Influence of normal load on indentation depth

#### 4.2 Normal load

Furthermore, it is evident that increasing the normal load allows an increase in the penetration depth. The linear dependence between the normal load and penetration depth was observed (**Fig. 4**). This relation was found for all orientations of the samples according to the rolling direction of the sheet metal. It also was found that the value of penetration depth for specific force value decreases non-linearly with the increase of sample pre-strain. This finding is a result of increasing deformation resistance due to the strain hardening phenomenon.

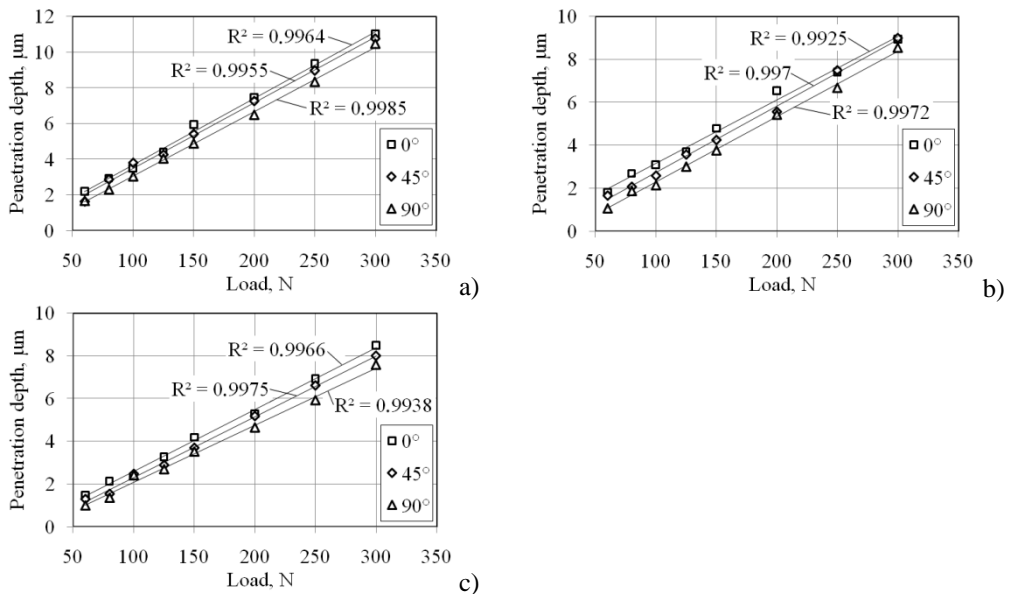


**Fig. 4** Effect of load on penetration depth value for pre-strained samples: a) 10%, b) 20%, c) 30%

For all pre-strained samples cut at  $0^\circ$  the indentation depths are smaller than in case of samples cut transverse to the rolling direction (**Fig. 5**). So, pre-strained samples cut transverse to the rolling direction exhibit higher deformation resistance than samples cut along the rolling direction. It is an effect of the anisotropic properties of the tested sheet metals. Despite the linear relationship between the normal load and penetration depth, the real contact area between the ball and sheet increases non-linearly with the penetration depth.

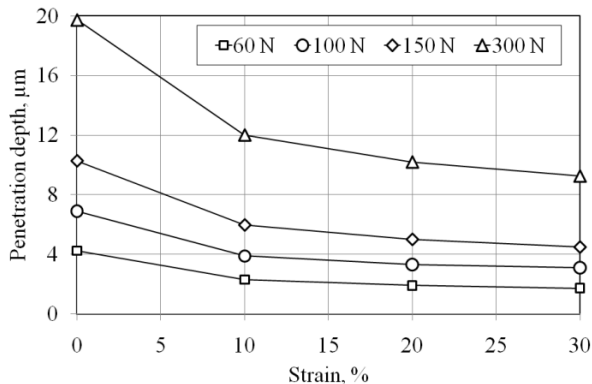


**Fig. 5** Effect of pre-strain value on penetration depth value

The evaluation of normal pressure in the case of small normal loads is a problematic issue because only the asperities of the roughness undergo a deformation (**Fig. 3**). The increasing of sample strain leads to the non-linear decreasing of the penetration depth. This relation is the result of the exponential character of Hollomon power-type law.

#### 4.3 Strain distribution

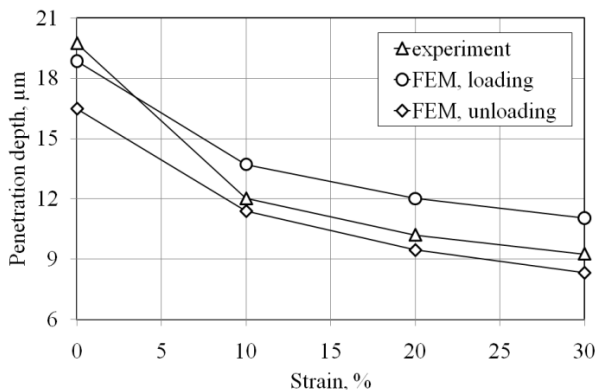


**Fig. 6** Comparison of penetration depths obtained in experiment and by numerical simulation

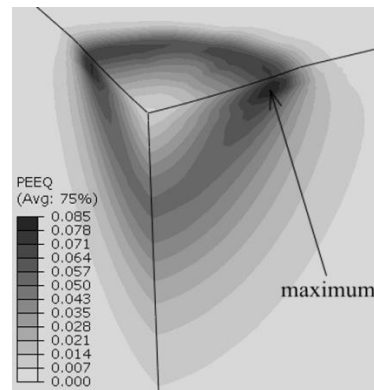


**Fig. 7** Distribution of equivalent plastic strain in non-prestrained sheet under load 300 N

The springback analysis is executed for studying the actual indentation depth after the indenter is unloaded. The numerical simulations were carried out for the maximal used load value (300 N). In the springback simulation, the material recovers its elastic deformation after the indenter is unloaded. The indentation depth after unloading is slightly smaller than the depth of the

indentation under loading (**Fig. 6**). The highest springback phenomenon is observed during indentation of non-prestrained sheet. If the sheet metal is pre-strained the springback is considerably lower due to strain hardening of material. The maximum value of equivalent plastic strain is found at the sub-surface, some distance below the centre of the contact region (**Fig. 7**). The anisotropy of material influenced the non-uniformity of the strain distribution around the line of axial symmetry of the model. It was clearly visible for higher values of ball indentations.

## 5 Conclusions

The relationship between the sample strain and roughness parameters Ra and Rz measured along the rolling direction of the sheet and transverse to the rolling direction is nearly linear.

The linear dependence between the normal load and the impression depth is observed. It was found that the value of penetration depth for specific force values decreases non-linearly with increasing material hardening.

The results of numerical simulations indicate that as the load increases, the plastic zone continues to grow until the edge of the plastic zone reaches the surface near the edge of the contact radius. The strain hardening effect on the springback phenomenon of the steel sheet plate after unloading was observed. The highest springback phenomenon is observed during indentation of non-prestrained sheet. If the sheet metal is pre-strained the springback is considerably lower due to strain hardening of material.

## References

- [1] S.D. Mesarovic, N.A. Fleck: *International Journal of Solids and Structures*, Vol. 37, 2000, No. 46-47, p. 7071-7091, DOI:10.1016/S0020-7683(99)00328-5
- [2] V.C. Sathish Gandhi, S. Ramesh, R. Kumaravelan, M. Thanmanaselvi: *Structural Engineering and Mechanics*, Vol. 44, 2012, No. 1, p. 61-72, DOI:10.12989/sem.2012.44.1.061
- [3] E. Evin, M. Tomaš, M. Kollárová, B. Antoszewski: *Acta Metallurgica Slovaca*, Vol. 20, 2014, No. 2, p. 189-199, DOI:10.12776/ams.v20i2.298
- [4] V. Boucly, D. Nélias, I. Green: *Journal of Tribology*, Vol. 129, 2007, No. 2, p. 235-245, DOI:10.1115/1.2464137
- [5] L. Ferrant Jr., R.W. Armstrong, N.N. Thadhani: *Materials Science and Engineering A*, Vol. 371, 2004, No. 1-2, p. 251-255, DOI:10.1016/j.msea.2003.12.003
- [6] J.L. Streater: *ASME Journal of Tribology*, 125, 2003, No. 1, p. 25-32, DOI:10.1115/1.1509772
- [7] V.C. Sathish Gandhi, R. Kumaravelan, S. Remesh: *Structural Engineering and Mechanics*, Vol. 52, 2014, No. 3, p. 469-483, DOI:10.12989/sem.2014.52.3.469
- [8] J.A. Greenwood, J.B.P. Williamson: *Proceedings of Royal Society of London. Series A*, Vol. 295, 1966, No. 1442, p. 300-319
- [9] J.R. Barber, M. Ciavarella: *International Journal of Solids and Structures*, Vol. 37, 2000, No. 1, p. 29-43, DOI:10.1016/S0020-7683(99)00075-X
- [10] V. Brizmer, Y. Kligerman, I. Etsion: *Tribology Letters*, Vol. 25, 2007, No. 1, p. 61-70, DOI:10.1007/s11249-006-9156-y
- [11] A. Ovcharenko, G. Halperin, G. Verberne, I. Etsion: *Tribology Letters*, Vol. 25, 2007, No. 2, 2007, p. 153-160, DOI:10.1007/s11249-006-9164-y
- [12] S. Shankar, M.M. Mayuram: *International Journal of Solids and Structures*, Vol. 45, 2008, No. 10, p. 3009-3020, DOI:10.1016/j.ijsolstr.2008.01.017

- [13] R.L. Jackson, I. Green: Tribology International, Vol. 39, 2006, No. 9, p. 906-914, DOI:10.1016/j.triboint.2005.09.001
- [14] B. Chatterje, P. Sahoo: Advances in Tribology, Vol. 212, 2012, p. 1-8, DOI:10.1155/2012/472794
- [15] W.R. Chang, I. Etsion, D.B. Bogy: Journal of Tribology, Vol. 109, 1987, No. 2, p. 257-263, DOI:10.1115/1.3261348
- [16] Y. Zhao, D.M. Maietta, L. Chang: Journal of Tribology, Vol. 122., 1999, No. 1, p. 86-93, DOI:10.1115/1.555332
- [17] C. Bagault, D. Nelias, M.C. Baietto: Journal of Tribology, Vol. 134, 2012, No. 3, p. 031401-1-031401-8
- [18] P. Sahoo, D. Adhikary, K. Saha: Journal of Tribology and Surface Engineering, Vol. 1, 2010, No. 1-2, p. 39-56
- [19] L. Kogut, I. Etsion: Journal of Applied Mechanics, Vol. 69, 2002, No. 5, p. 657-662, DOI:10.1115/1.1490373
- [20] R.L. Jackson, I. Green: Journal of Tribology, Vol. 127, 2005, No. 2, p. 343-354, DOI:10.1115/1.1866166
- [21] D.K. Leu: Journal of Mechanical Science and Technology, Vol. 26, 2011, No. 6, 1509-1517, DOI:10.1007/s12206-011-0134-4
- [22] T. Trzepieciński: Archives of Civil and Mechanical Engineering, Vol. 10, 2010, No. 4, p. 95-106, DOI:10.1016/S1644-9665(12)60035-1
- [23] T. Trzepieciński, H.G. Lemu: International Journal of Material Forming, Vol. 4, 2011, No. 4, p. 357-369, DOI:10.1007/s12289-010-0994-7
- [24] R. Hill: Proceedings of the Royal Society of London. Series A, Vol. 193, 1948, No. 1033, p. 281-297
- [25] T. Trzepieciński, A. Bazan, H.G. Lemu: Applied Mechanics and Materials, Vol. 789-790, 2015, p. 3-6, DOI:10.4028/www.scientific.net/AMM.789-790.3
- [26] F. Stachowicz: Acta Mechanica, Vol. 226, 2015, p. 3651-3662, DOI:10.1007/s00707-015-1416-1
- [27] R. Quey, P.R. Dawson, J.H. Driver: Journal of the Mechanics and Physics of Solids, vol. 60, 2012, No. 3, p. 509-524, DOI:10.1016/j.jmps.2011.11.005

### Acknowledgements

*The research leading to these results has received funding from the People Programme (Marie Curie International Research Staff Exchange) of the European Union's FP7/2007-2013/ under REA grant agreement n° PIRSES-GA-2013-610547.*